Distance-dependent cellular palmitoylation of de-novo-designed sequences and their translocation to plasma membrane subdomains

Inmaculada Navarro-Lérida[1], Alberto Álvarez-Barrientos[2], Francisco Gavilanes[1] and Ignacio Rodriguez-Crespo[1],*

[1]Departamento de Bioquímica y Biología Molecular, Facultad de Ciencias Químicas, Universidad Complutense, 28040 Madrid, Spain
[2]Fundación Centro Nacional de Investigaciones Cardiovasculares Carlos III, Madrid, Spain
*Author for correspondence (e-mail: nacho@bbm1.ucm.es)

Summary

Using recursive PCR, we created an artificial protein sequence that consists of a consensus myristoylation motif (MGCTLS) followed by the triplet AGS repeated nine times and fused to the GFP reporter. This linker-GFP sequence was utilized as a base to produce multiple mutants that were used to transfect COS-7 cells. Constructs where a 'palmitoylable' cysteine residue was progressively moved apart from the myristoylation site to positions 3, 9, 15 and 21 of the protein sequence were made, and these mutants were used to investigate the effect of protein myristoylation on subsequent palmitoylation, subcellular localization, membrane association and caveolin-1 colocalization. In all cases, dual acylation of the GFP chimeras correlated with translocation to Triton X-100-insoluble cholesterol/sphingomyelin-enriched subdomains. Whereas a strong Golgi labeling was observed in all the myristoylated chimeras, association with the plasma membrane was only observed in the dually acylated constructs. Taking into account the conflicting data regarding the existence and specificity of cellular palmitoyl-transferases, our results provide evidence that de-novo-designed sequences can be efficiently S-acylated with palmitic acid in vivo, strongly supporting the hypothesis that non-enzymatic protein palmitoylation can occur within mammalian cells. Additionally, this palmitoylation results in the translocation of the recombinant construct to low-fluidity domains in a myristate-palmitate distance-dependent manner.

Key words: Myristoylation, Caveolin, Palmitoylation, Rafts, Subcellular targeting

Introduction

Covalent attachment of both myristic and palmitic acid to the N-terminus of cellular proteins, most of which are involved in signaling events, occurs more widely than previously recognized (Dunphy and Linder, 1998; Resh, 1999). For instance, the α subunits of heterotrimeric G proteins (Milligan et al., 1995; Wedegaerten et al., 1995), the myristoylated palmitoylated serine/threonine protein kinase (MPSK) (Berson et al., 1999), endothelial nitric oxide synthase (eNOS) (Robinson et al., 1995; Liu et al., 1995), a-kinase anchoring protein 18 (AKAP18) (Fraser et al., 1998) and members of the Src family of tyrosine kinases (Koegl et al., 1994; Resh, 1994) are irreversibly acylated by myristic acid and reversibly acylated by palmitic acid. Whereas myristoylation occurs at the free amino group of the first Gly residue resulting in the formation of an amide bond, palmitoylation takes place through the formation of a thioester bond with the side chain of an internal Cys residue. The biochemistry of protein myristoylation, as well as the properties of N-myristoyl transferase (the enzyme that catalyzes the transfer of myristate from myristoyl-CoA to the free amino group of a Gly residue of proteins), are well understood (Bhatnagar et al., 1999). However, the palmitoylation of previously myristoylated proteins at the side chains of cysteine residues in proximity to the N-terminus end of proteins is a less well understood process, and both enzymatic and non-enzymatic mechanisms of palmitic acid transfer have been proposed so far (Dunphy and Linder, 1998; Resh, 1999). In the majority of the cases studied to date, dually acylated proteins are regulated through a palmitoylation-depalmitoylation cycle that correlates with a transient association-dissociation from cholesterol-sphingolipid-enriched subdomains present in the cellular membrane (Milligan et al., 1995; Dunphy and Linder, 1998; McCabe and Berthiaume, 1999; Simons and Toomre, 2000).

The partial purification of enzyme activities responsible for palmitoylation of Gα subunits (Dunphy et al., 1996), N-Ras (Liu et al., 1996b) and the C-terminal regions of *Drosophila* Ras1 and Ras2 (Ueno and Suzuki, 1997) has been reported. However, whereas the former enzymatic activity remains elusive because of problems with cloning and molecular characterization (Dunphy et al., 2001), the other two palmitoyl transferase activities turned out to be a peroxisomal 3-oxoacyl-CoA thiolase (Liu et al., 1996a) and a transferase that did not depend upon the previous prenylation of the peptide that was used as a substrate (Ueno and Suzuki, 1997), a feature that is required for Ras palmitoylation in vivo (Hancock et al., 1989).

Very recently, skinny Hedgehog (*ski*), a *Drosophila* acyltransferase that is able to catalyze the palmitoylation of Hedgehog (*Hh*), has been identified (Chamoun et al., 2001). However, it has been reported that the palmitoyl group is attached to the N-terminus of Hedhehog on the α amino group of Cys-24 (Pepinsky et al., 1998). This attachment originates through an autoproteolytic cleavage at an internal site during which the bioactive N-terminal product of cleavage acquires a C-terminally bound cholesterol molecule. Consequently, it remains to be seen whether the mammalian orthologs of this acyltransferase are able to catalyze the incorporation of palmitic acid to other cellular targets.

Additional acyltransferase activities have been observed and partially characterized in erythrocyte ghosts and placental membranes (Das et al., 1997; Schmidt et al., 1995; Veit et al., 1998) as well as in brain lysates (Berthiaume and Resh, 1995), although all of them remain refractory to molecular cloning and full characterization.

Conversely, Duncan and Gilman showed that palmitoyl-CoA can stoichiometrically palmitoylate previously myristoylated Giα1 in vitro in the absence of any cellular acyltransferase with kinetics for the palmitoylation reaction that resemble those described for palmitoylation in vivo (Duncan and Gilman, 1996). The non-enzymatic palmitoylation of Gsα at Cys3 was also reported (Mollner et al., 1998). Magee and coworkers very elegantly showed that myristoylated N-terminal peptides from the *Yes* protein tyrosine kinase, but not their non-myristoylated counterparts, could be non-enzymatically palmitoylated by palmitoyl-CoA in vitro (Bañó et al., 1998). The palmitoylation reaction was pseudo-enzymatic in the sense that it depended not only on the previous myristoylation of the substrate but also on the length of the incubation period, the temperature and the substrate concentration. Consequently, apparent K_m and V_{max} values could be estimated for the peptide substrate. Other examples of non-enzymatic acylation of proteins reported in the literature include UDP-glucuronosyl transferase from rat liver (Yamashita et al., 1995), the myelin proteolipid (Bizzozero et al., 1987) and rhodopsin (O'Brien et al., 1987), as well as cysteine-containing peptides (Quesnel and Silvius, 1994).

To investigate whether the cellular transfer of palmitate from palmitoyl-CoA could occur in a de-novo-designed protein sequence, we constructed a polypeptide where a consensus N-myristoylation hexapeptide was followed by the triplet Ala-Gly-Ser repeated nine times and fused to GFP. We referred to this construct as 'linker-GFP'. We avoided any basic residue such as Lys or Arg within this sequence pattern since that would also promote membrane targeting and raft localization (McCabe and Berthiaume, 1999). Four of the Ser residues in our construct, with a six-residue spacing within them and located at different distances from the N-terminus, were substituted by Cys residues (Fig. 1), and their phenotypes were analyzed. Additionally, 12 residues were introduced between the last cysteine residue that can be putatively palmitoylated (Cys21) and the GFP sequence in order to rule out the possibility that the three-dimensional fold of the GFP might interfere with the palmitoylation processes. Our data are consistent with the hypothesis that in vivo palmitoylation of proteins can take place as long as a reactive cysteine residue is in proximity to the cellular membrane.

Materials and Methods

Cell culture and materials

COS-7 cells were grown in Dulbecco's modified Eagle's medium (DMEM) supplemented with 10% foetal bovine serum (FBS), 100 u/ml penicillin, 100 µg/ml streptomycin and 2 mM L-glutamine in a 5% CO_2 atmosphere at 37°C. Transient transfection with the various plasmids was performed using Superfect Transfection Reagent (Qiagen) following the manufacturers' instructions. The cells were typically analyzed 36 hours post transfection. The Giα1-EGFP (enhanced green fluorescent protein) construct was a generous gift from Marco Parenti (University of Milano-Bicocca). It contains five mutations (F64C, S65T, V163A, I167T and S175G) that result in increased fluorescence emission. Anti-caveolin-1 antibodies were obtained from Transduction Laboratories (Heidelberg, Germany) (rabbit polyclonal and mouse monoclonal 2234). The anti-Gqα and the anti-integrin β1 antibodies were from Calbiochem (Schwalbech, Germany). The anti-5′-nucleotidase antibody was a gift from M. A. Lizarbe (Complutense University, Madrid, Spain). A commercial anti-GFP polyclonal antibody was obtained from Clontech; additionally, we raised a rabbit anti-GFP antiserum after injection of purified recombinant GFP in rabbits. BODIPY-TR-ceramide was from Molecular Probes. [9, 10-^{3}H]-Palmitic acid (40-60 Ci/mmol), [9, 10-^{3}H]-Myristic acid (40-60 Ci/mmol), Protein A-Sepharose and Cy3-labeled anti-rabbit antibodies were from Amersham Pharmacia Biotech. All other biochemicals used were of the highest purity available and were obtained from regular commercial sources.

Construction of the GFP fusion proteins

The general design of the nine mutants described herein consisted of N-terminal tags fused to the enhanced GFP using a *Bss*HII site in the pCDNA3 plasmid (Invitrogen, Barcelona, Spain) under the control of the cytomegalovirus promoter. We performed recursive PCR in order to obtain a de-novo-designed sequence using six overlapping oligonucleotides and introducing a *Nco*I site at the 5′ end and a *Bss*HII site at the 3′ end of the desired sequence. This starting sequence, referred to as linker-GFP, consisted of a consensus myristoylation motif (MGCTLS) followed by the triplet AGS repeated nine times followed by the GFP sequence, that is MGCTLS-(AGS)9-GFP (Fig. 1). Site-directed mutagenesis was employed in order to introduce the desired mutations. In the case of the eNOS-GFP construct, we amplified the first 55 residues of endothelial nitric oxide synthase, introducing novel *Nco*I and *Bss*HII sites at the 5′ and 3′ end, respectively. This first 55 residues of eNOS include the myristoylation site together with the two palmitoylated cysteines (Cys15 and Cys26) and is enough to target GFP to Golgi regions and discrete regions of the plasma membrane (Liu et al., 1997). PCR-amplified bands of all the constructs were ligated into the pGEM-T vector (Invitrogen), and they were subsequently sequenced. Owing to the presence of *Nco*I and *Bss*HII sites in pCDNA3, we first double digested the Giα1(32 aa)-GFP construct with *Eco*RI plus *Xba*I and ligated the excised fragment into the corresponding sites of a pUC vector polylinker. All the pGEM-T vectors with linker-GFP, G2A-GFP, C3S-GFP, G2A/C3S-GFP, C3S/S9C-GFP, C3S/S15C-GFP, C3S/S21C-GFP and eNOS-GFP were then double digested with *Nco*I plus *Bss*HII, and the excised band was subsequently ligated into the corresponding site of pUC-Giα1(32 aa)-GFP. Finally, all the constructs in pUC were double digested with *Eco*RI plus *Xba*I and the excised bands ligated in the corresponding sites in pCDNA3. Finally, every plasmid was sequenced to confirm the desired mutations.

Immunoblot analysis and cellular fractionation

Cellular proteins were resolved by 15% acrylamide SDS-PAGE and transferred to nitrocellulose membranes. Western blots were incubated for 2 hours in PBS containing 2% powdered skimmed milk. Subsequently, the nitrocellulose membranes were incubated overnight

with the primary antibodies (typically 1:1000 in PBS), washed and finally incubated for 2 hours with a horseradish-peroxidase-conjugated goat anti-rabbit antibody (Pierce). Detection was performed using a ECL detection kit (Amersham Pharmacia Biotech). Quantification of the intensity of the bands was performed using a UViband V97 software (UVItec St. John's Innovation Centre, Cambridge, UK).

Fractionation was performed by harvesting the cells and resuspending them in 0.4 ml of PBS supplemented with 1 mM EDTA, 10 μg/ml aprotinin, 10 μg/ml leupeptin and 2 mM phenylmethylsulfonyl fluoride (Sigma) as protease inhibitors. The cellular suspensions were then passed several times through a syringe (0.5×16 mm) and were further homogenized with short sonication cycles (3×10 seconds each) on ice. Unbroken cells and cellular debris were eliminated by a 10 minute centrifugation at 3000 g in a table-top microcentrifuge. The samples were then centrifuged for 16 hours at 200,000 g in a SW65 rotor (Beckman) at 4°C. The cellular pellets (particulate fraction) and the supernatants (soluble fraction) were brought up to equal volumes and subsequently analyzed by SDS-PAGE followed by immunodetection with a rabbit anti-GFP antibody.

Metabolic labeling and immunoprecipitation

COS-7 cells transiently transfected with the desired construct were starved for 1 hour with DMEM in the absence of any FBS 36 hours after transfection. The monolayers were subsequently labeled for 4 hours with 200 μCi [9, 10-^{3}H]-myristic acid or 200 μCi [9, 10-^{3}H]-palmitic acid. The radioactive compounds were dried completely under nitrogen and resuspended initially in 10 μl of DMSO followed by 1 ml of DMEM containing 2% dialyzed FBS plus 0.5% de-fatted BSA (Sigma). The cells were washed with PBS, scraped and lysed in Ripa buffer (10 mM Tris, 150 mM NaCl, 1% Triton X-100, 0.1% SDS, 0.1% deoxicholate, pH 7.35) in the presence of protease inhibitors. After centrifugation of the cell lysate at 6000 g for 10 minutes at 4°C, the supernatant was incubated with 10 μl of the rabbit anti-GFP antibody. The mixture was incubated overnight at 4°C, and then 25 μl of a 1:1 suspension of Sepharose:Protein A-Sepharose beads (Amersham Pharmacia Biotech) was added to each sample and the incubation was maintained for 5 hours at 4°C. Immunoprecipitates were centrifuged at 16,000 g in a table top microcentrifuge for 10 minutes, and the supernatant was removed. Immunoprecipitates were then washed twice in 0.5 ml of ice-cold Ripa buffer. Samples were separated by SDS-PAGE, and the gels were treated with Enhance solution (Amersham Pharmacia Biotech) in order to improve the radioactivity signal. The gels were dried in a BioRad vacuum apparatus and exposed on photography films in a cassette for 4 weeks at –80°C.

Confocal fluorescence microscopy

Transiently transfected COS-7 cells grown on 0.2% gelatin-coated glass coverslips were washed two times with PBS and fixed for 15 minutes at room temperature with freshly prepared 2% paraformaldehyde in PBS. The stock paraformaldehyde solution was prepared at 4% in PBS and was centrifuged at 16,000 g for 5 minutes at room temperature in a table-top microcentrifuge in order to remove insoluble material prior to dilution. After removal of the 2% paraformaldehyde solution, the cells were washed with PBS and incubated with cold methanol at –20°C for 10 more minutes. The methanol was removed, and the coverslips were allowed to dry for 5 minutes. Then, the cells were washed with PBS and the slides were mounted using Fluoroguard anti-fade reagent (BioRad). The subcellular localization was observed under a BioRad MRC-1024 confocal microscope equipped with two lasers using the excitation wavelength of 488 nm for the GFP intrinsic fluorescence and 543 nm for the Cy3 fluorophore and the BODIPY-TR-ceramide. Double labeling was performed on transiently transfected COS-7 cells

permeabilized with methanol. Incubation with a rabbit polyclonal anti-caveolin-1 antibody (Transduction) was done for 1 hour at 37°C in a wet chamber. Next, the cells were washed with PBS and the anti-rabbit Cy3-labeled secondary antibody was added. BODIPY-TR-ceramide (1.5 μM in DMEM) staining was done in vivo in COS-7 transfected cells, and the reagent was added 30-60 minutes before analysis of the double labeling under the confocal microscope. The live cells were washed twice with PBS and examined for their subcellular distribution. Fixing was avoided, since the methanol significantly distorts the BODIPY-TR-ceramide signal. When the in vivo fluorescence measurements were done (incubations with β-methylcyclodextrin), the cells were kept at 37°C using a Peltier system, and Hepes buffer was used all throughout the experiment. The cycloheximide treatment (100 μg/ml) was performed 24 hours post-transfection for 2 hours at 37°C.

Preparation of caveolin-enriched low density membrane fractions

Typically, four transiently transfected COS-7 confluent 75 cm^2 flasks were scraped and the cells resuspended into 2 ml (final volume) of Mes buffered saline (MBS) (25 mM MES, pH 6.5, 0.15 M NaCl, 1 mM PMSF plus 1% Triton X-100) at 4°C. Isolation of the Triton-X-100-insoluble fractions with a lower number of cells needed the amount of detergent to be scaled down proportionally. Homogenization of the cells was carried out with a minimum of 10 strokes through a syringe (0.5×16 mm) on ice. The homogenate was then adjusted to 40% sucrose by the addition of 2 ml of 80% sucrose prepared in MBS (4 ml in total), and it was placed at the bottom of a Beckman SW40 13 ml Ultraclear tube. The discontinuous gradient (40-30-5%) was formed by loading 4 ml of 30% sucrose followed by 4 ml of 5% sucrose always in MBS. Separation was performed at 200,000 g for 18 hours in a SW40 rotor (Beckman) at 4°C. A light scattering band confined to the interface of the 5-30% sucrose region was observed that contained the majority of the caveolin-1 protein and excluded most of the cellular proteins. After centrifugation, 1 ml fractions were collected from the bottom of the tube to yield a total of 12 fractions. After that, 1 ml of cold acetone was added to each tube and the homogenous mixture was allowed to precipitate overnight at 4°C. The samples were centrifuged at 16,000 g in a microcentrifuge, and the protein pellets were allowed to dry for 2 hours to assure the complete elimination of acetone traces. The protein precipitates were then analyzed by SDS-PAGE. In addition to caveolin-1, 5′-nucleotidase, a GPI-anchored protein was also used as a protein marker of caveolin-1-enriched low fluidity subdomains (Kenworthy and Edidin, 1998). The amount of total protein in each fraction was measured using a micro-Lowry method. In essence, we first incubated the protein sample with 2.5 ml of reagent E (25 ml NaOH, 0.2 M plus 25 ml 4% carbonate mixed with 250 μl 1% copper sulfate and 250 μl of 2% tartrate). After 10 minutes of reaction at room temperature, we added 250 μl of Folin reagent and let the mixture stand for an additional 30 minutes. Absorbance was determined at 750 and 500 nm, and the values were interpolated in a calibration curve performed with known quantities of bovine serum albumin.

Co-immunoprecipitation

Transiently transfected COS-7 cells were washed twice with PBS, scraped and lysed with several strokes of a thin-gauge syringe in Ripa buffer in the presence of protease inhibitors on ice. Samples were clarified for 1 hour at 4°C using 20 μl of a 1:1 mixture of Sepharose:Protein-A-sepharose. After clarification, the supernatants were incubated with 10 μl of the primary antibody (anti-GFP or anti caveolin-1) overnight at 4°C. Then, 20 μl of the Sepharose:Protein-A-sepharose slurry was added and the mixture was incubated for 2 additional hours at 4°C. The samples were centrifuged in a table-top microcentrifuge, and the immunoprecipitates were then washed twice

in 0.5 ml of ice-cold Ripa buffer. The resin beads were subsequently boiled in SDS-PAGE loading buffer and processed in a 15% acrylamide gel. The SDS-PAGE gel was afterwards transferred to nitrocellulose, and the membrane was probed with the desired antibodies.

Results

Design, transient expression in COS-7 cells and acylation of the tagged-GFP constructs

We created various constructs to address the intriguing possibility that de novo-designed sequences can become palmitoylated in vivo. In addition, we investigated whether cellular palmitoylation is dependent on the distance of the reactive cysteine from the N-terminus of the protein. With that in mind, we envisaged a protein sequence with a myristoylation consensus motif (MGCTLS) followed by a 'palmitoylable' cysteine residue, which could be progressively moved apart from the myristoyl moiety (Fig. 1A). Fusion of this N-terminal tag to the soluble GFP was expected to result in constructs where the membrane-interacting properties, incorporation of myristic and palmitic acids and subcellular localization is dictated by the N-terminal extension (van't Hof and Resh, 2000). A similar approach has been utilized for other acylated proteins (Liu et al., 1997; Galbiati et al., 1999; McCabe and Berthiaume, 1999; Martín-Belmonte et al., 2000; Michaelson et al., 2001). We refer to the construct with the consensus myristoylation site and a cysteine residue at position 3 as 'linker-GFP', and it was used as a template for various other mutant constructs. By PCR mutagenesis we introduced an alanine residue at position 2 (G2A-GFP mutant), a serine residue at position 3 (C3S-GFP mutant), the double mutant with alanine at position 2 plus serine at position 3 (G2A/C3S-GFP mutant), and three mutants with serine at position 3 and cysteine at positions 9, 15 or 21 (C3S/S9C-GFP, C3S/S15C-GFP and C3S/S21C-GFP mutants). Additionally, we created a construct fusing the first 55 residues of eNOS to GFP to be used together with a Giα1(32 residues)-GFP plasmid as positive controls of dual acylation with myristic and palmitic acids. As expected, transient transfection of COS-7 cells with the various pCDNA3 plasmids containing the chimeric GFP cDNAs resulted in similar level of expression for all of the recombinant proteins (Fig. 1B).

Metabolic radiolabeling of the GFP chimeras was performed using [9, 10-^{3}H]-myristic acid or [9, 10-^{3}H]-palmitic acid followed by immunoprecipitation of the cell lysates with the anti-GFP antibody (Fig. 1C). As expected, GFP alone was neither myristoylated nor palmitoylated, whereas every GFP chimera that possessed the N-terminal Gly in the context of a consensus myristoylation sequence (Ser residue at position 6) efficiently incorporated myristic acid (linker, C3S, C3S/S9C, C3S/S15C, C3S/S21C and eNOS-GFP chimeras). Predictably, mutation of Gly2 to Ala2 resulted in no myristic acid incorporation (G2A-GFP and G2A/C3S-

GFP chimeras) (Fig. 1C). Efficient incorporation of palmitic acid occurred in the constructs linker-GFP, C3S/S9C-GFP and C3S/S15C-GFP as well as in the positive control eNOS-GFP (in addition to the Giα1-GFP construct) (data not shown). Under identical conditions, a faint band of radioactivity appeared for the C3S/S21C-GFP chimera, which is indicative of a very low level of incorporation of palmitate at position 21 (Fig. 1C). Quantification of this band using the UVI-band software revealed that 18% of the linker-GFP construct had been incorporated. Non-myristoylated mutant G2A-GFP was unable to be palmitoylated in spite of the fact that it contains a Cys residue at position 3. Consequently, efficient S-acylation can occur at positions Cys3 (linker-GFP), Cys9 (C3S/S9C-GFP), Cys15 (C3S/S15C-GFP) and in minimal amounts at Cys21 (C3S/S21C-GFP) but always in previously myristoylated polypeptides. Since the four 'palmitoylable' Cys residues (Cys3, Cys9, Cys15 and Cys21) were surrounded by identical amino acids, we must conclude that only the distance to the N-terminus of the GFP chimera is a determinant for protein palmitoylation. We could rule out the possibility that the lower incorporation of palmitic acid at position 21 is caused by its proximity to the GFP sequence, since 12 amino acids have been introduced between Cys21 and the first residue of GFP. Previous studies have shown that cysteine residues located either five (Fyn kinase-GFP construct) or seven amino acids from the GFP reporter (GAP43-GFP construct) were efficiently palmitoylated (McCabe and Berthiaume, 1999). Note that the myristoylated C3S-GFP construct, which lacks any cysteine residue in the linker region, is unable to become palmitoylated at any of the
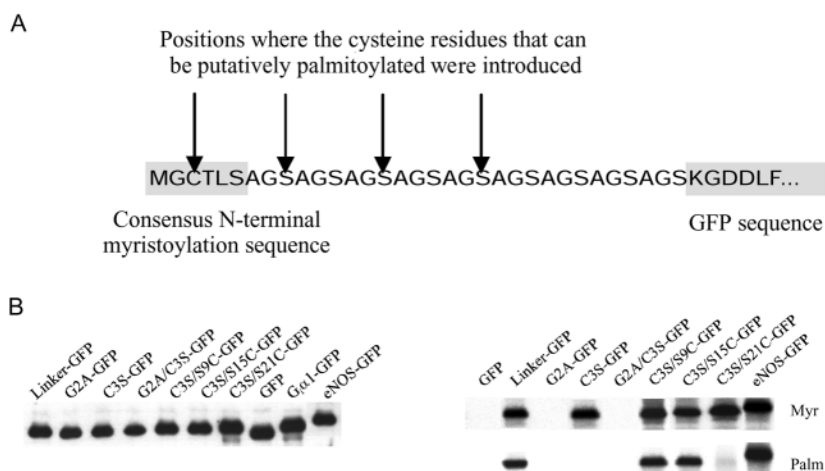

Fig. 1. Illustration of the linker-GFP construct with the location of the consensus myristoylation sequence and the positions where the mutations were introduced (A), expression of the recombinant proteins in COS-7 cells (B) and fatty acylation of the GFP chimeras (C). By recursive PCR, the triplet AGS repeated nine times was created following a consensus N-myristoylation sequence and fused in frame to the GFP sequence. Mutations were introduced at Gly2, Cys3, Ser9, Ser15 and Ser21 in various combinations, as described in the Materials and Methods (A). The different linker-GFP constructs were inserted in a pCDNA3 vector that was used to transfect COS-7 cells (B). Transfected COS-7 cells were starved for 1 hour in DMEM without serum and were then metabolically labeled for 4 hours with either [^{3}H]-myristic acid (Myr) or [^{3}H]-palmitic acid (Palm). Cell lysates were immunoprecipitated with an anti-GFP antibody, analyzed by SDS-PAGE and exposed to a film as described in the Materials and Methods. Identical results were obtained in two independent metabolic labeling experiments.

Cys residues present in the GFP sequence itself (Cys48 and Cys70) (Fig. 1C).

Subcellular localization of the GFP chimeras by confocal microscopy

To assess whether the N-terminal extensions confer different subcellular localization information, we transfected COS-7 cells with the various GFP constructs and inspected their distribution using laser confocal microscopy (Fig. 2). The linker-GFP mutant displays a plasma-membrane and focal perinuclear localization with nuclear exclusion and low cytosolic levels of fluorescence. This phenotype contrasts with the subcellular distribution of GFP alone, which produces both cytosolic and a marked nuclear staining; thus linker-GFP distribution strongly suggests that the acylation of the linker-GFP construct is responsible for the observed subcellular targeting. Substitution of the Gly residue at position 2 by Ala (G2A-GFP and G2A/C3S-GFP chimeras), a mutation known to impede myristoylation (Fig. 1C), restores the widespread cytosolic and nuclear distribution, with negative staining of nucleoli observed for GFP alone. Elimination of the putative palmitoylation site Cys3 and maintaining the myristoylation site (C3S-GFP mutant) results in a distribution characterized by the nuclear exclusion and the loss of the plasma membrane staining, with an enrichment in intracellular membranes, in perinuclear vesicles as well as in the ER (Fig. 2). The myristoylated and palmitoylated GFP chimeras C3S/S9C, C3S/S15C as well as the two positive controls of dual acylation (Giα1 and eNOS) display a similar staining to the linker-GFP construct; that is, plasma membrane plus distinctive intracellular vesicular organelles and a complete nuclear exclusion. Finally, the myristoylated C3S/S21C-GFP chimera, which incorporates palmitic acid very poorly, exhibits a mixed phenotype reflecting both the linker-GFP and C3S-GFP construct localizations (Fig. 2).

Fig. 2. Subcellular localization of the various constructs characterized in the present work as visualized by laser confocal microscopy. COS-7 cells were transfected with the various constructs, and the fluorescence was analyzed 36 hours after transfection. GFP fluorescence was visualized by confocal microscopy at an excitation wavelength of 488 nm. Bar, 50 μm.

Membrane partitioning of the GFP chimeras

To investigate the effect of the various acylation states on the membrane partitioning of the GFP chimeras, we fractionated the cellular lysates into Supernatant (S-soluble) and Pellet (P-membrane-associated) fractions after ultracentrifugation at 200,000 *g* (Fig. 3). The presence of the GFP chimeras was detected using specific antibodies, and the intensity of the bands was accurately determined using a UViband V97 software. Constructs that did not incorporate either myristic or palmitic acid, such as GFP, G2A-GFP and G2A/C3S-GFP, were predominantly soluble. Dually acylated GFP chimeras, such as linker, C3S/S9C, C3S/S15C, Giα1 and eNOS,
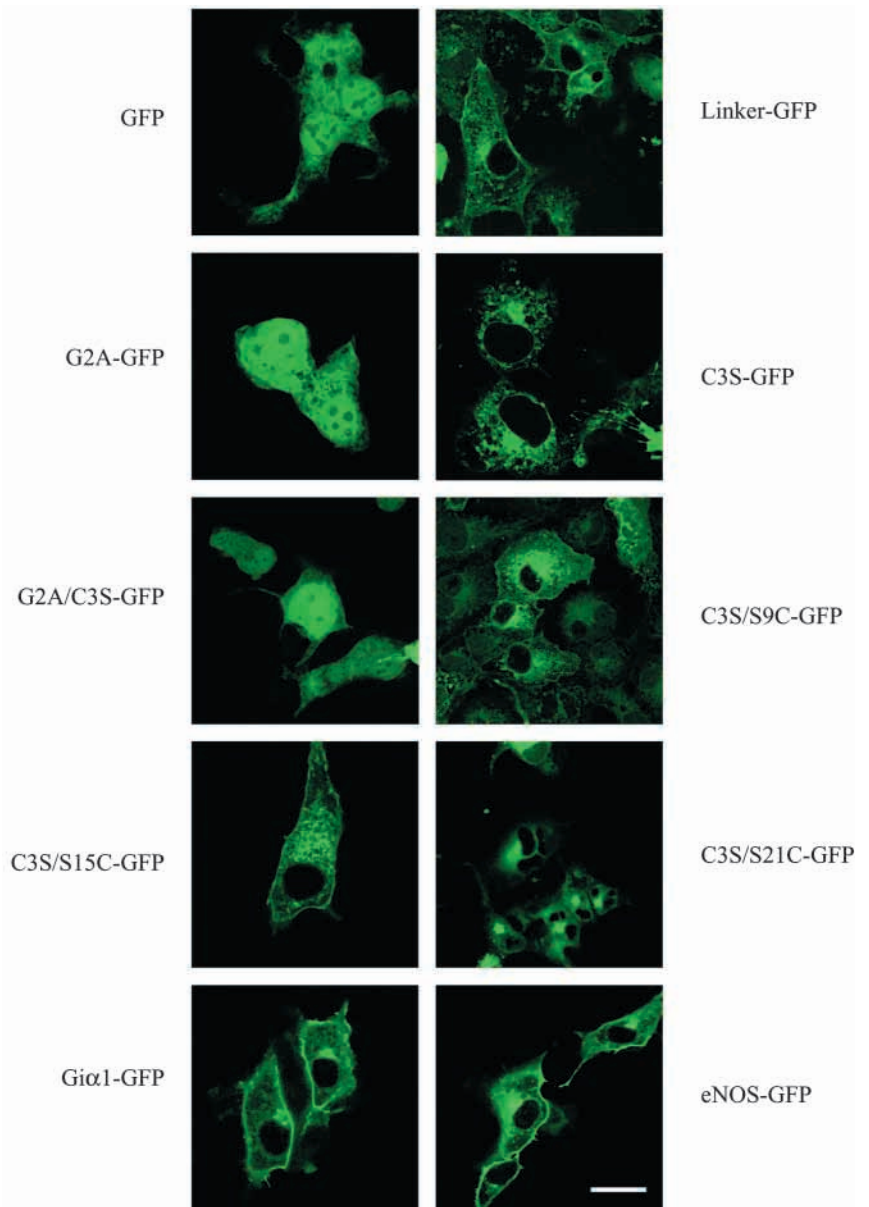
partitioned preferentially into the membrane-associated fractions. (More than 65% of the chimeras were in membrane-bound fractions; Fig. 3.) The construct C3S-GFP, which is myristoylated but not palmitoylated, has approximately half of its total immunoreactive protein in each fraction, and an almost identical distribution is also observed in the case of the C3S/S21C-GFP chimera. Therefore, as expected, N-terminal myristoylation increases the overall hydrophobicity of the engineered GFP chimeras, resulting in an increased association with cellular membranes (roughly 50% in the P lane), whereas the additive effect of myristoylation plus palmitoylation results in the majority of the protein associating with the membrane (Fig. 3).
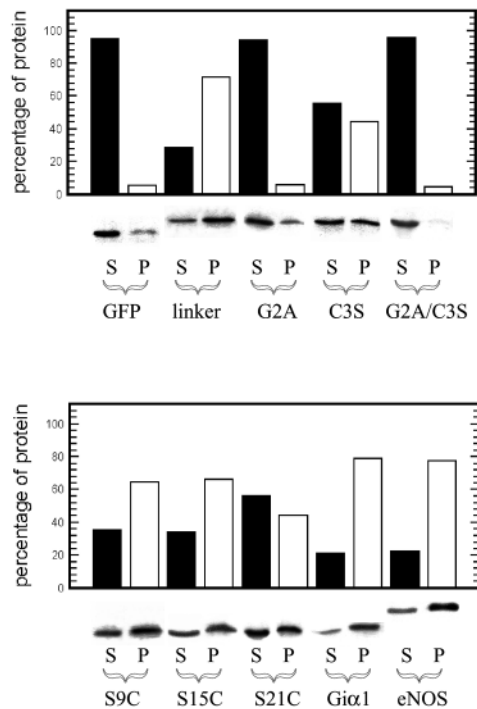
Fig. 3. Subcellular fractionation of COS-7 cells expressing the various GFP constructs. Transfected COS-7 were lysed and after clarification of the cellular debris by centrifugation were fractionated into supernatant (S) and pellet (P) fractions by ultracentrifugation for 16 hours at 200,000 g as described in the Materials and Methods. The fractions were subjected to SDS-PAGE, analyzed by western blot with an antibody against GFP, and the resulting bands were quantified using UVIband V97 software. These results are representative of a minimum of five independent fractionations, with less than 5% variation among different experiments.

Fig. 4. Sucrose flotation gradients in the presence of Triton X-100. COS-7 cells transfected with the GFP-tagged constructs were extracted in the presence of Triton X-100 at 4°C and subjected to centrifugation on a 40:30:5% sucrose gradient as described in the Materials and Methods. After centrifugation, the gradient tubes were divided into 12 equal aliquots collected from the bottom and analyzed by SDS-PAGE and western blotting. The amount of protein in each sample was determined using a micro-Lowry method (upper panel; average distribution). Similar results were obtained in four independent experiments.

Enrichment of the GFP chimeras in Triton-insoluble membrane rafts

Owing to their elevated cholesterol and sphingolipids content, caveolar membranes are resistant to extraction at 4°C by nonionic detergents such as Triton X-100; instead they float on bottom-loaded sucrose density gradients (Kurzchalia and Parton, 1999; Simons and Toomre, 2000). We inspected the targeting of the various acylated constructs to these low-fluidity domains preparing 40:30:5% sucrose discontinuous gradients in the presence of Triton X-100 following a well-defined procedure (Lisanti et al., 1999). Caveolin-1, which is endogenously expressed in COS-7 cells, together with 5′-nucleotidase, a GPI-anchored protein, was used as a marker for these Triton-X100-insoluble domains (Kenworthy and Edidin, 1998; Lisanti et al., 1999; Kurzchalia and Parton, 1999). Partial (but not complete) localization of the GFP chimeras to these caveolin-1-enriched domains was only observed for the dually acylated constructs linker-GFP, C3S/S9C-GFP, C3S/S15C-GFP, Giα1-GFP and eNOS-GFP (Fig. 4). The non-acylated GFP, G2A-GFP and G2A/C3S-GFP proteins were found in fractions 1 through 4 (bottom of the gradient), where most of the cellular proteins were present (upper panel). Although both the myristoylated C3S-GFP and C3S/S21C-GFP chimeras had a certain tendency to float towards lower density fractions (they were present in fractions 1 through 7), they were not
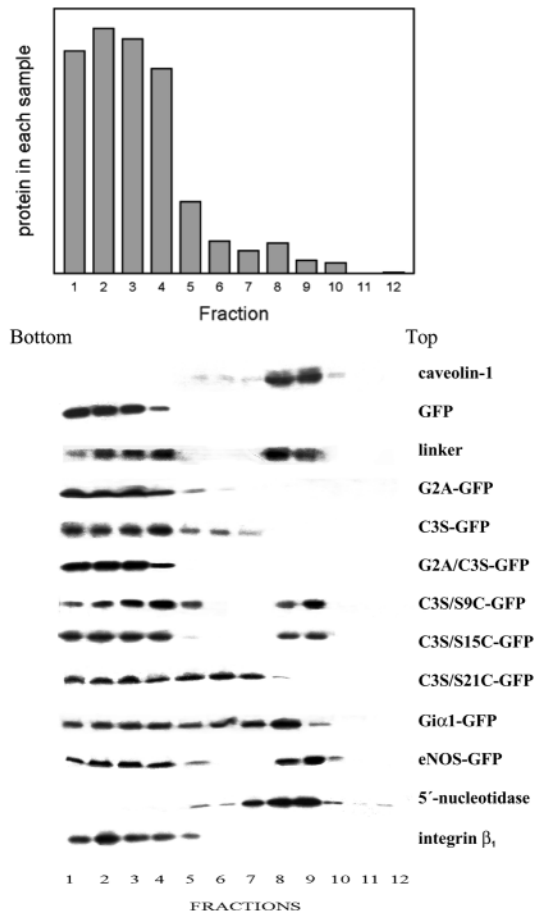
significantly enriched in fractions 8 and 9 accompanying caveolin-1. Thus, the myristic acid moiety alone confers membrane-interacting properties but not the capacity to fully interact with the low-fluidity cholesterol-sphingomyelin enriched domains. Additionally, we used the integrin β_1, a transmembrane protein known to be excluded from Triton-X100-insoluble rafts (Nusrat et al., 2000) as a specific marker of membrane-associated but caveolae-excluded protein. Integrin β_1 is concentrated in high-density fractions (40% sucrose, fractions 1-4) at the bottom of the tube (Fig. 4).

Confocal microscopy colocalization studies of the GFP chimeras with caveolin-1 in transfected COS-7 cells

Next, we investigated whether the subcellular localization of the various GFP chimeras transfected in COS-7 cells partially overlapped with that of endogenous caveolin-1 (Fig. 5A). Transiently transfected COS-7 cells were permeabilized and

incubated with anti-caveolin-1 antibodies. The three mutant GFP chimeras shown on Fig. 5A, linker-GFP, G2A-GFP and C3S-GFP, are representative of each of the well defined phenotypes. Taking advantage of the GFP intrinsic fluorescence, together with signal emitted from the Cy3-labeled secondary antibodies, we inspected the colocalization of the three chimeras with caveolin-1 that are present endogenously in COS-7 cells. Caveolin-1 staining was mostly focal and punctate, and it could be observed in regions close to the plasma membrane and to a lesser degree in intracellular aggregates; it was always excluded from the cell nucleus (Fig. 5, middle panels). When merged with the GFP signal (Fig. 5, right panels; see also supplemental data), there was a significant overlap (yellow) in distribution with the linker-GFP and G2A-GFP chimeras at areas close to the plasma membrane (arrows) and no overlap with the C3S chimera. However, the dually acylated mutant linker-GFP still exhibited extensive GFP fluorescence in cytosolic regions where the caveolin-1 fluorescence was excluded. A similar codistribution with caveolin-1 in the plasma membrane and adjacent areas (caveolae) was observed for the other dually acylated GFP chimeras (data not shown). The coincidence in the fluorescence signal of the G2A-GFP chimera with caveolin-1 was somehow expected, since this mutant presents GFP fluorescence in the entire cytoplasm and nucleus. Interestingly, the merge of the myristoylated, non-palmitoylated C3S-GFP chimera signal with that of caveolin-1 reveals a crown-like distribution. Whereas caveolin-1 distribution is centered on plasma membrane areas, the C3S-GFP fluorescence is selectively excluded from them.

Intriguingly, dually acylated N-terminal segments of Giα1 could still associate with caveolin-1 and translocate to the plasma membrane in spite of the fact that they lack the caveolin-1-interacting motif (Galbiati et al., 1999). To determine whether the targeting to Triton-X100-insoluble domains as well as the localization of our tagged GFP constructs to caveolae coincided with a physical interaction between the recombinant proteins and caveolin-1, we performed co-immunoprecipitation experiments (Fig. 5B). Immunoprecipitation of linker-GFP or C3S-GFP transiently transfected COS-7 cells with anti-caveolin-1 antibodies, and analysis of the immunoprecipitate with anti-GFP antibodies failed to reveal any positive interaction.
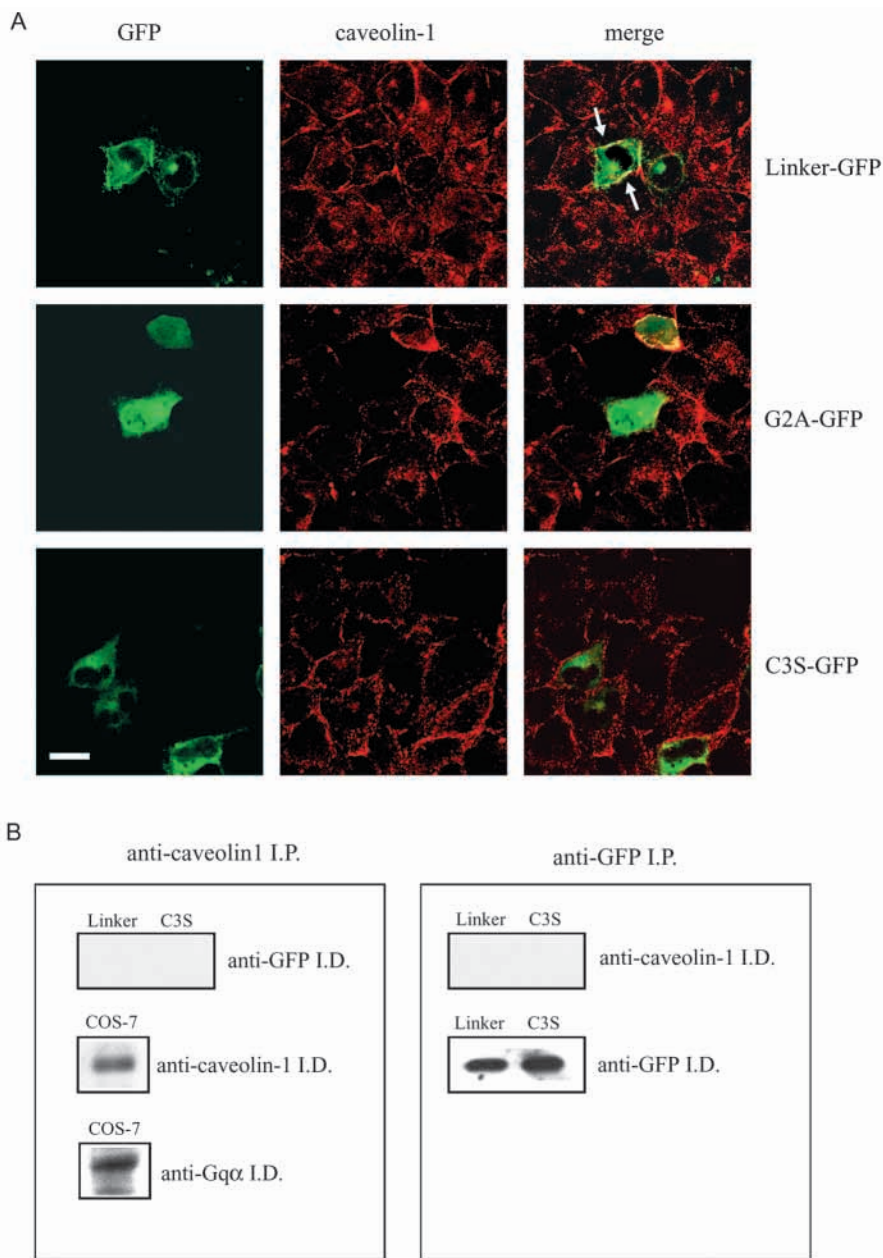

Fig. 5. Colocalization studies of linker-GFP, G2A-GFP and C3S-GFP with caveolin 1. COS-7 cells were transfected with the linker-GFP (upper panels), G2A-GFP (middle panels) or C3S-GFP (lower panels) constructs and analyzed 36 hours post-transfection (A). The GFP fluorescence (left panels) was obtained after excitation at 488 nm, whereas the Cy3 fluorescence (middle panels) was obtained after excitation at 543 nm. The right panels show the merge of both fluorescence signals. Bar, 50 μm. The physical interaction of caveolin-1 with the GFP chimeras was analyzed in pull-down experiments (B). COS-7 cells transfected with the linker-GFP construct, C3S-GFP construct or mock-transfected were lysed and immunoprecipitated with anti-caveolin-1 antibodies (left panel) or with anti-GFP antibodies (right panel) as described in the Materials and Methods. The immunoprecipitated samples were then analyzed (immunodetected, I.D.) with anti-GFP, anti-caveolin-1 or anti-Gqα antibodies as outlined in the figure.

Nevertheless, we were able to detect caveolin-1 as well as a caveolae-associated protein (the α subunit of Gq) in caveolin-1-immunoprecipitated COS-7 cells (Fig. 5B, left panel). Likewise, when we immunoprecipitated linker-GFP or C3S-

GFP-transfected COS-7 cells with anti-GFP antibodies, identification of caveolin-1 association in the immunoprecipitate was unsuccessful (Fig. 5B, right panel). By contrast, experiments performed in parallel confirm that the immunoprecipitation of the GFP constructs was successful. Hence, the most likely explanation for our results is that dual acylation per se partially targets the GFP reporter to caveolae owing to the intrinsic low-fluidity properties of this cholesterol-sphingomyelin-enriched domain, rather than to a physical interaction with caveolin-1 in COS-7 cells.

Colocalization of chimeric GFPs with the Golgi compartment

To assess whether the various N-terminal fatty acylated sequences contain different subcellular information that might target the GFP chimeras to the Golgi apparatus, we used BODIPY-Texas Red-ceramide in vivo as a marker. The intrinsic fluorescence of the linker-GFP, G2A-GFP and C3S-GFP chimeras in living cells together with the Golgi staining is shown in Fig. 6. Internalization of this Golgi marker occurs via endocytosis, and some of the endosome and areas of the trans Golgi network can display partial labeling, particularly in our in vivo staining. The three GFP-tagged constructs colocalize with the Golgi marker in intracellular membranes adjacent to the nucleus (Fig. 6A, right panels). Colocalization of the linker-GFP chimera with BODIPY-TR-ceramide is more apparent in perinuclear regions, although partial overlap can also be observed in certain endocytic regions in the proximity of the plasma membrane. On the other hand, the broad distribution of the G2A-GFP fluorescence in the entire cytosol and nucleus without any specific staining invalidates any positive colocalization with the Golgi marker. Mutant C3S-GFP exhibits a clear overlap with BODIPY-TR-ceramide, which indicates that the myristoylation observed for this mutant results in Golgi targeting. Additionally, we inspected the phenotype adopted by the linker-GFP and C3S-GFP chimeras upon incubation with cycloheximide for 2 hours (Fig. 6B). In both cases, the total fluorescence observed diminishes. Significantly, in the dually acylated linker-GFP construct, the plasma-membrane-associated signal is considerably less affected than the Golgi localization. Hence, this Golgi pool probably reflects a biosynthetic intermediate of the linker-GFP mutant along the secretory pathway en route to the caveolae-associated plasma membrane subdomains. In the case of the C3S-GFP mutant, the Golgi staining becomes significantly reduced, whereas
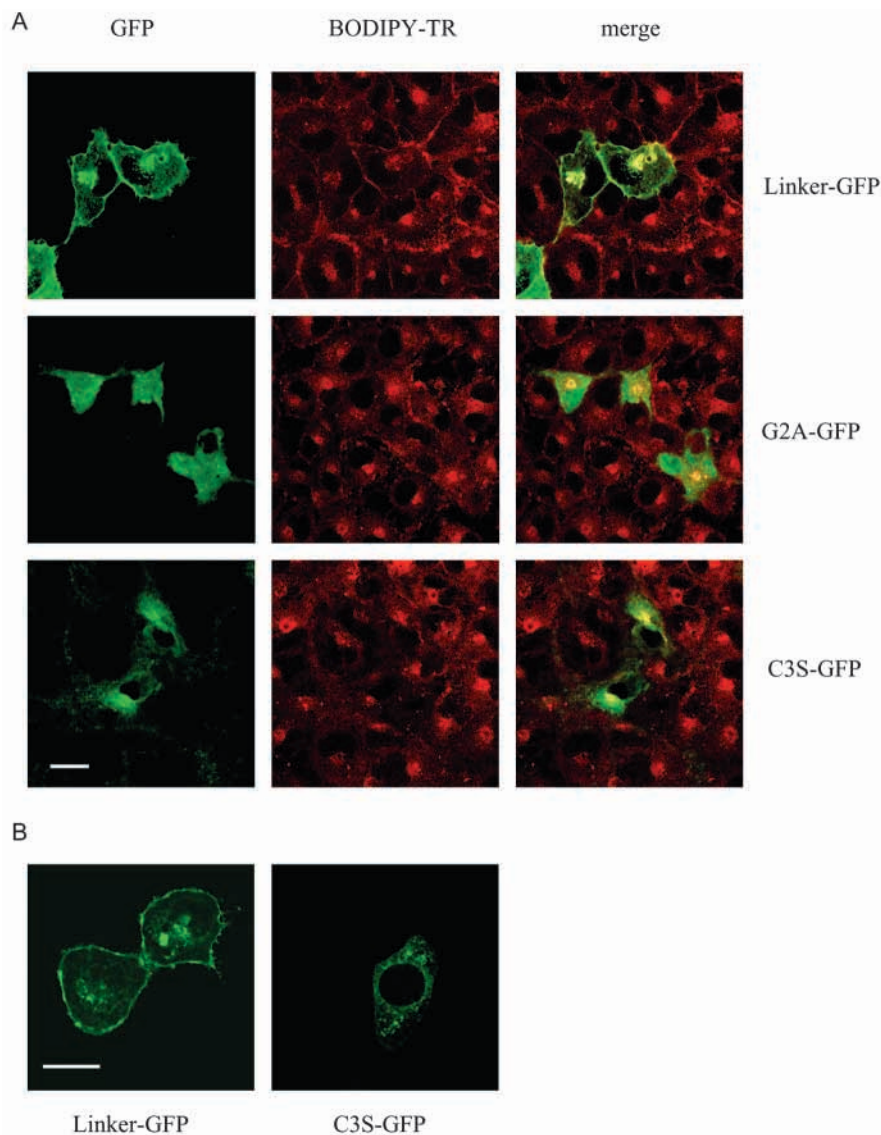

Fig. 6. Colocalization studies of linker-GFP, G2A-GFP and C3S-GFP with the Golgi marker BODIPY-TR-ceramide (A) and cycloheximide treatment of the linker-GFP and C3S-GFP chimeras (B). (A) COS-7 cells were transfected with the linker-GFP (upper panels), G2A-GFP (middle panels) or C3S-GFP (lower panels) constructs and, 36 hours post-transfection, they were incubated with the Golgi apparatus marker BODIPY-Texas Red-ceramide (1.5 µM in DMEM). The GFP fluorescence (left panels) was obtained after excitation at 488 nm whereas the Texas Red fluorescence (middle panels) was obtained after excitation at 543 nm. Right panels show the merge of both fluorescence signals. Bar, 50 µm. (B) Changes induced in the localization of the linker-GFP and C3S-GFP mutants upon treatment with 100 µg/ml cycloheximide for 2 hours. The treatment was performed 24 hours post-transfection.

some ER-associated perinuclear staining is still observed (Fig. 6B).

Changes induced in the subcellular localization of the GFP chimeras induced by cholesterol depletion and by 2-bromopalmitate treatment

We also investigated whether in vivo cholesterol depletion with β-methyl cyclodextrin alters the plasma membrane targeting of the dually acylated chimera linker-GFP (Fig. 7). Inspection of
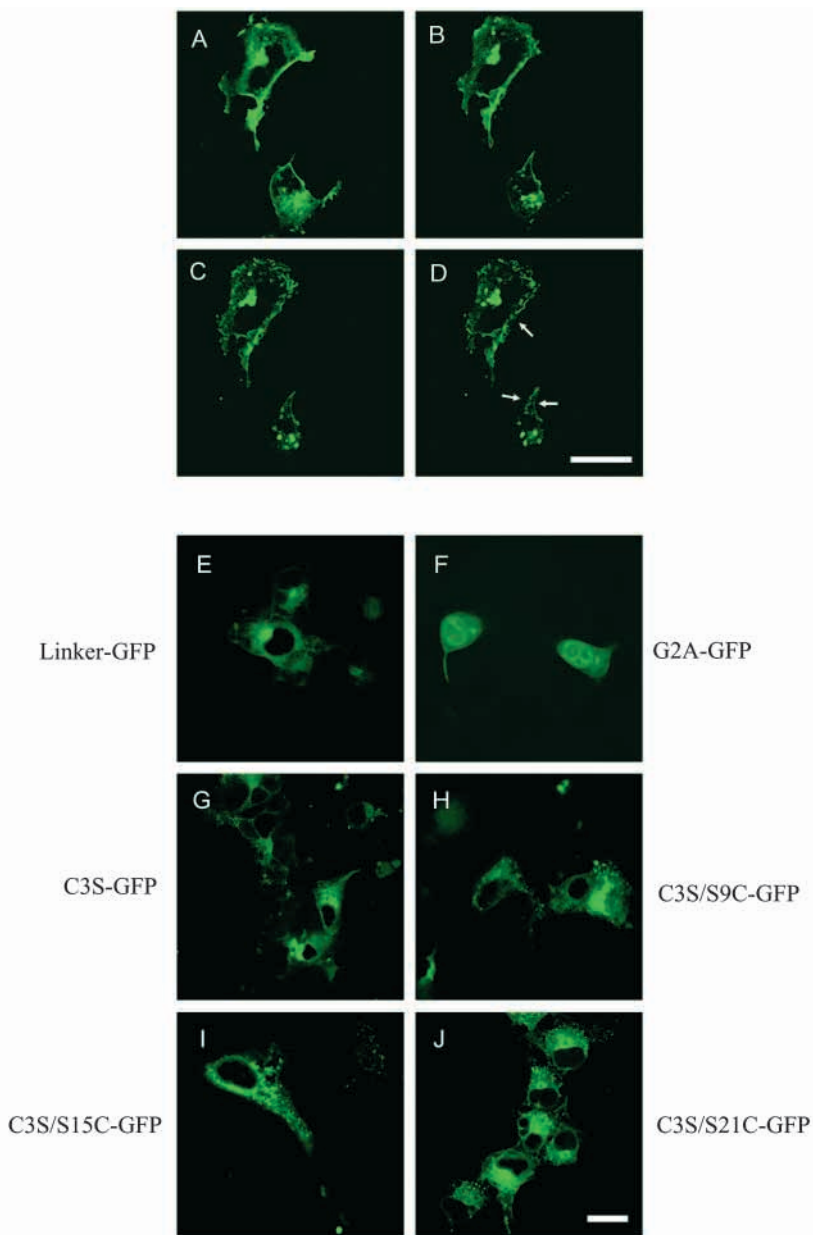
Fig. 7. In vivo changes in the subcellular localization of the linker-GFP construct upon cholesterol depletion using β-methyl cyclodextrin and changes in the subcellular localization of various GFP chimeras upon incubation with 2-bromopalmitate. COS-7 cells were transfected with the linker-GFP plasmid and incubated with 10 mM β-methyl cyclodextrin for 0, 10, 20 or 30 minutes (A-D) at 36 hours after transfection. Arrows in D denote changes in the plasma membrane fluorescence. COS-7 cells were also transfected with the linker-GFP, G2A-GFP, C3S-GFP, C3S/S9C-GFP, C3S/S15C-GFP or C3S/S21C-GFP plasmids and, 36 hours post-transfection, incubated with 25 μM 2-bromopalmitate for 16 hours (E-J). Bar, 50 μm.

the mutant is taking place owing to the sequestration of cholesterol. Whereas the perinuclear Golgi staining remains basically unaffected by treatment for 30 minutes with the reagent, most of the plasma membrane localization of the myristoylated and palmitoylated mutant is profoundly modified (Fig. 7D, arrows). Thus, after dual acylation and partial translocation to plasma membrane subdomains, the integrity of the cholesterol-sphingomyelin rafts appears to be requisite for the correct caveolar association of the dually acylated construct.

Recently, 2-bromopalmitate was reported to be an effective inhibitor of protein palmitoylation in vivo (Webb et al., 2000). Therefore, we used this reagent to further confirm the role of palmitoylation in the membrane targeting of the dually acylated GFP chimeras (Fig. 7E-J). As expected, the linker-GFP, C3S/S9C-GFP and C3S/S15C-GFP chimeras were significantly affected by the 2-bromopalmitate treatment, resulting in phenotypes that strongly resembled that of the C3S-GFP chimera, with most of the plasma membrane localization being lost. The G2A-GFP and C3S-GFP chimeras remained unaffected by the treatment (Fig. 7), as did the G2A/C3S-GFP construct (data not shown). Intriguingly, the reagent also affected the fluorescence associated with intracellular membranes, resulting in increased vacuolization, which lead to the appearance of small vesicles that display trapped GFP fluorescence. This phenotype could be observed both in the singly myristoylated (C3S-GFP, C3S/S21C-GFP) as well as in the dually acylated chimeras and very probably reflects some collateral metabolic alteration induced by 2-bromopalmitate treatment. However, treatment of COS-7 cells with bromopalmitate or methyl-cyclodextrin under identical conditions did not affect the plasma membrane staining of integrin $\alpha_3\beta_1$, a protein known to be excluded from rafts/caveolae (data not shown).

Discussion

In general, myristoylated cellular proteins, although more hydrophobic than their non-myristoylated counterparts, have barely enough energy to translocate from the cytosol to the inner leaflet of the plasma membrane. In this regard, a 10^{-4} M effective dissociation constant calculated for myristoylated peptides and liposomes was deduced from the 8 kcal/mol energy requirement needed to carry out this process (Peitzsch and McLaughlin, 1993). Consequently, in order to bind tightly to membranes, myristoylated proteins are often palmitoylated or possess basic or apolar residues at their N-terminus that promote their interaction with lipids (Milligan et al., 1995; Dunphy and Linder, 1998; Resh, 1999; McCabe and Berthiaume, 1999).

the changes arising from cholesterol removal in COS-7 cells 36 hours post-transfected with the linker-GFP chimera revealed that after 10 minutes of incubation with β-methyl cyclodextrin, the GFP fluorescence associated with the plasma membrane was altered (Fig. 7B). Examination of the live COS-7 cells at 20 and 30 minutes after treatment (Fig. 7C,D) allows us to conclude that a redistribution of the caveolar targeting of

Although some myristoylated proteins possess free sulfhydrils alongside its primary sequence, only the cysteines located at the N-terminus of the protein incorporate palmitic acid. Interestingly, palmitoylation of previously myristoylated proteins often leads to the translocation of the dually acylated protein to cholesterol-sphingomyelin-enriched subdomains (Dunphy and Linder, 1998; Resh, 1999; Melkonian et al., 1999; Galbiati et al., 1999).

To date, the mechanisms underlying cellular protein palmitoylation have remained elusive despite the significant number of identified proteins that are post-translationally modified through the attachment of a palmitic moiety to the side chain of a cysteine residue. Unlike the well characterized myristoylation motif recognized by the enzyme N-myristoyl transferase, inspection of the N-terminus of dually acylated proteins reveals that no clear consensus sequence exists for a certain protein for S-acylation with palmitic acid. Although some palmitoylated cysteine residues are in the proximity of basic residues (for example, in Hck and Fgr kinases and $G\alpha_z$), a few others are close to Ser or Thr residues (for example, in Lck kinase, $G\alpha_{i1}$, $G\alpha_0$ and Vac8p) or hydrophobic residues (Fyn, Lyn and Yes kinases, AKAP18, MPSK and eNOS). Remarkably, myristoylation is frequently a prerequisite for a dually acylated protein to become palmitoylated, since elimination of the myristic acid aceptor residue, Gly2, abrogates subsequent palmitoylation (Koegl et al., 1994; McCabe and Berthiaume, 1999; Galbiati et al., 1999). The putative existence of a unique cellular palmitoyl transferase presupposes that this enzyme must recognize cysteine residues inserted within different amino acid motifs before catalyzing the addition of palmitate from palmitoyl-CoA. Moreover, this enzyme should selectively recognize a very vague sequence motif present only in a myristoylated substrate and subsequently transfer palmitic acid to the thiol group of a proximal Cys residue. Conversely, multiple palmitoyl transferases might exist, each with a different cellular substrate, implicated individually in the tight regulation of the activity of one dually acylated protein, many of which are involved in signaling processes (Milligan et al., 1995; Dunphy and Linder, 1998; Simons and Toomre, 2000; Janes et al., 2000).

However, since the palmitoylation-depalmitoylation recycling of proteins is a strictly regulated process, one can envisage that this cycle might be controlled at the depalmitoylation level (Dunphy and Linder, 1998; Resh, 1999). Interestingly, a cytoplasmic acyl-protein thioesterase (APT-1) that removes palmitate from G protein α subunits, p21Ras and eNOS has been recently identified (Duncan and Gilman, 1998; Yeh et al., 1999), although the cellular mechanisms of regulation of this esterase remain to be established. Since APT-1 also hydrolyzes both free palmitoyl-CoA and palmitic acid covalently bound to proteins, it is conceivable that an increase in cellular APT-1 activity is accompanied by both diminished protein palmitoylation and augmented protein depalmitoylation. Nevertheless, further experiments seem necessary in order to analyze the cellular mechanisms that regulate protein acylation.

In this study, we have analyzed whether de-novo-designed sequences fused to the GFP reporter become effectively palmitoylated in vivo. Two other dually acylated GFP-tagged chimeras - Giα1 and eNOS - were used as positive controls.

In the absence of hydrophobic residues, polybasic signals or prenylation sites, the palmitoylation of a Cys residue inserted in the linker-GFP chimera is a direct consequence of its reactivity towards cellular palmitoyl transferases (enzymatic palmitoylation) or its direct interaction with Pal-CoA (non-enzymatic palmitoylation). Efficient palmitoylation was observed at Cys3, Cys9, Cys15 and marginally at position Cys21, which is indicative that (i) palmitoylation can efficiently occur in a de novo-designed sequence, (ii) this process is dependent on the proximity of the reactive thiol to the N-terminus of the protein and (iii) palmitoylation only takes place on sequences that were previously myristoylated. The degree of palmitoylation observed was similar to the one displayed by the eNOS-GFP chimera under identical pulse treatment (Fig. 1C). It is interesting, in this context, to note that eNOS becomes N-terminally myristoylated and subsequently palmitoylated at positions Cys15 and Cys26 (Liu et al., 1995; Robinson et al., 1995). However, the presence of multiple hydrophobic residues in the proximity of these palmitoylated cysteine residues are probably responsible for the attachment of the palmitate in such distant positions, since mutagenesis of the five Leu residues present within residues 16 and 25 of eNOS abrogate palmitoylation (Liu et al., 1997).

According to our data, myristoylation is a prerequisite for protein palmitoylation (Fig. 1C), mimicking the well known dependence of S-acylation on prior membrane association via myristoyl, prenyl or transmembrane peptide moieties (Dunphy and Linder, 1998; Resh, 1999). Whereas N-terminal myristoylation is enough to induce the nuclear exclusion and partial intracellular membrane association of the GFP reporter, dually acylated proteins are excluded from the cell nucleus and localize to intracellular Golgi membranes and partially to the plasma membrane (Fig. 2). Although both myristoylation and palmitoylation individually increased the partitioning of the proteins into membranous fractions, the dually acylated proteins were found almost uniquely in the particulate fractions (Fig. 3). The increased hydrophobicity provided by both post-translational acylations resulted in augmented interaction with cellular membranes, although only palmitoylation conferred on the GFP chimeras the ability to translocate towards cholesterol-sphingomyelin-enriched domains, in accordance with the proposed role of palmitoylation and caveolae localization (Figs 4 and 5). Indeed, plasma membrane staining of the dually acylated, but not the myristoylated, GFP chimeras provides support for the unique lipid-interacting properties endowed by the palmitic moiety (Fig. 5). Since our constructs lack the consensus caveolin-1-interacting motif (Couet et al., 1997), it must be concluded that palmitate per se conveys on the N-terminal tag the ability to interact with Triton-insoluble, low-fluidity domains. Significantly, in spite of the colocalization with caveolin-1 in plasma membrane locations (Fig. 5), dually acylated chimeras were unable to physically interact with caveolin-1. This lack of physical interaction with caveolin-1 has also been observed in short stretches of dually acylated kinases fused to the GFP reporter as well (McCabe and Berthiaume, 2001).

N-terminal myristoylation was sufficient to colocalize the GFP chimeras with the Golgi marker BODIPY-TR-ceramide, whereas dual acylation lead to both Golgi targeting and partial colocalization with caveolin-1 (Figs 5 and 6). The coincidence

with the caveolin-1 staining for our myristoylated plus palmitoylated chimeras occurs mostly in the proximity of the plasma membrane, although, as expected (Luetterforst et al., 1999), some Golgi staining could also be observed. Further demonstration of the localization of the dually acylated constructs to Triton-insoluble membrane subdomains was achieved using the cholesterol-sequestering agent β-methyl-cyclodextrin and 2-bromopalmitate, a known inhibitor of cellular palmitoylation (Fig. 7).

Interestingly, recent studies carried out with surfactant protein C, a small protein that contains a polar palmitoylated segment followed by a long transmembrane stretch, have demonstrated that S-acylation is strongly dependent on the distance of the palmitoylable cysteine residue from the hydrophobic transmembrane α-helix (ten Brinke at al., 2002). In this context, cysteine residues that are positioned in proximity to the transmembrane domain are more efficiently palmitoylated than those separated by a greater distance.

Finally, although our data cannot rule out the existence of cellular palmitoyl transferase activities, they are consistent with the hypothesis that certain cellular proteins are non-enzymatically S-acylated, especially if the reactive cysteine thiol is in the proximity of the membrane environment owing to a previous lipidic modification (myristoylation or prenylation). In our case, if palmitoylation was the result of an enzymatic activity, we must then assume that a cellular palmitoyl-transferase is able to recognize a non-cellular N-terminal sequence (designed de novo). Alternatively, since approximately 10% of the cellular palmitoyl-CoA is bound to membranes in COS-7 cells (Bañó et al., 1998), it is then conceivable that the direct transfer of palmitate to a reactive cysteine residue might take place. The recent discovery that Src family tyrosine kinases, Gα subunits, GAP43 and Ras can become heterogeneously acylated on cysteine residues with fatty acids other than palmitate (Liang et al., 2001) also supports the suggestion that non-enzymatic palmitoylation of proteins might be occurring within cells. Since the thiol of a cysteine is a good nucleophile, the selective incorporation of one fatty acid over the other might depend on the availability of the specific membrane-bound acyl-CoAs in the proximity of the reactive cysteine.

References

Bañó, M. C., Jackson, C. S. and Magee, A. I. (1998). Pseudo-enzymatic S-acylation of a myristoylated yes protein tyrosine kinase peptide in vitro may reflect non-enzymatic S-acylation in vivo. *Biochem. J.* **330**, 723-731.

Berson, A. E., Young, C., Morrison, S. L., Fujii, G. H., Sheung, J., Wu, B., Bolen, J. B. and Burkhardt, A. L. (1999). Identification and characterization of a myristylated and palmitylated serine/threonine protein kinase. *Biochem. Biophys. Res. Commun.* **259**, 533-538.

Berthiaume, L. and Resh, M. D. (1995). Biochemical characterization of a palmitoyl acyltransferase activity that palmitoylates myristoylated proteins. *J. Biol. Chem.* **270**, 22399-22405.

Bhatnagar, R. S., Futterer, K., Waksman, G. and Gordon, J. I. (1999). The structure of myristoyl-CoA:protein N-myristoyltransferase. *Biochim. Biophys. Acta.* **1441**, 162-172.

Bizzozero, O. A., McGarry, J. F. and Lees, M. B. (1987). Autoacylation of myelin proteolipid protein with acyl coenzyme A. *J. Biol. Chem.* **262**, 13550-13557.

Chamoun, Z., Mann, R. K., Nellen, D., von Kessler, D. P., Bellotto, M., Beachy, P. A. and Basler, K. (2001). Skinny hedgehog, an acyltransferase required for palmitoylation and activity of the hedgehog signal. *Science* **293**, 2080-2084.

Couet, J., Li, S., Okamoto, T., Ikezu, T. and Lisanti, M. P. (1997). Identification of peptide and protein ligands for the caveolin-scaffolding domain. Implications for the interaction of caveolin with caveolae-associated proteins. *J. Biol. Chem.* **272**, 6525-6533.

Das, A. K., Dasgupta, B., Bhattacharya, R. and Basu, J. (1997). Purification and biochemical characterization of a protein-palmitoyl acyltransferase from human erythrocytes. *J. Biol. Chem.* **272**, 11021-11025.

Duncan, J. A. and Gilman, A. G. (1996). Autoacylation of G protein alpha subunits. *J. Biol. Chem.* **271**, 23594-23600.

Duncan, J. A. and Gilman, A. G. (1998). A cytoplasmic acyl-protein thioesterase that removes palmitate from G protein alpha subunits and p21(RAS). *J. Biol. Chem.* **273**, 15830-15837.

Dunphy, J. T. and Linder, M. E. (1998). Signalling functions of protein palmitoylation. *Biochim. Biophys. Acta* **1436**, 245-261.

Dunphy, J. T., Greentree, W. K., Manahan, C. L. and Linder, M. E. (1996). G-protein palmitoyltransferase activity is enriched in plasma membranes. *J. Biol. Chem.* **271**, 7154-7159.

Dunphy, J. T., Greentree, W. K. and Linder, M. E. (2001). Enrichment of G-protein palmitoyltransferase activity in low density membranes: in vitro reconstitution of Galphai to these domains requires palmitoyltransferase activity. *J. Biol. Chem.* **276**, 43300-43304.

Fraser, I. D., Tavalin, S. J., Lester, L. B., Langeberg, L. K., Westphal, A. M., Dean, R. A., Marrion, N. V. and Scott, J. D. (1998). A novel lipid-anchored A-kinase Anchoring Protein facilitates cAMP-responsive membrane events. *EMBO J.* **17**, 2261-2272.

Galbiati, F., Volonte, D., Meani, D., Milligan, G., Lublin, D. M., Lisanti, M. P. and Parenti, M. (1999). The dually acylated NH2-terminal domain of gi1alpha is sufficient to target a green fluorescent protein reporter to caveolin-enriched plasma membrane domains. Palmitoylation of caveolin-1 is required for the recognition of dually acylated G-protein alpha subunits in vivo. *J. Biol. Chem.* **274**, 5843-5850.

Hancock, J. F., Magee, A. I., Childs, J. E. and Marshall, C. J. (1989). All ras proteins are polyisoprenylated but only some are palmitoylated. *Cell* **57**, 1167-1177.

Janes, P. W., Ley, S. C., Magee, A. I. and Kabouridis, P. S. (2000). The role of lipid rafts in T cell antigen receptor (TCR) signalling. *Semin. Immunol.* **12**, 23-34.

Kenworthy, A. K. and Edidin, M. (1998). Distribution of a glycosylphosphatidylinositol-anchored protein at the apical surface of MDCK cells examined at a resolution of <100 A using imaging fluorescence resonance energy transfer. *J. Cell Biol.* **142**, 69-84.

Koegl, M., Zlatkine, P., Ley, S. C., Courtneidge, S. A. and Magee, A. I. (1994). Palmitoylation of multiple Src-family kinases at a homologous N-terminal motif. *Biochem. J.* **303**, 749-753.

Kurzchalia, T. V. and Parton, R. G. (1999). Membrane microdomains and caveolae. *Curr. Opin. Cell. Biol.* **11**, 424-431.

Liang, X., Nazarian, A., Erdjument-Bromage, H., Bornmann, W., Tempst, P. and Resh, M. D. (2001). Heterogeneous fatty acylation of Src family kinases with polyunsaturated fatty acids regulates raft localization and signal transduction. *J. Biol. Chem.* **276**, 30987-30994

Lisanti, M. P., Sargiacomo, M. and Scherer, P. E. (1999). Purification of caveolae-derived membrane microdomains containing lipid-anchored signaling molecules, such as GPI-anchored proteins, H-Ras, Src-family tyrosine kinases, eNOS, and G-protein alpha-, beta-, and gamma-subunits. *Methods Mol. Biol.* **116**, 51-60.

Liu, J., García-Cardeña, G. and Sessa, W. C. (1995). Biosynthesis and palmitoylation of endothelial nitric oxide synthase: mutagenesis of palmitoylation sites, cysteines-15 and/or -26, argues against depalmitoylation-induced translocation of the enzyme. *Biochemistry* **34**, 12333-12340.

Liu, L., Dudler, T. and Gelb, M. H. (1996a). Purification of a protein palmitoyltransferase that acts on H-Ras protein and on a C-terminal N-Ras peptide. *J. Biol. Chem.* **271**, 23269-23276.

Liu, L., Dudler, T. and Gelb, M. H. (1996b). Purification of a protein

palmitoyltransferase that acts on H-Ras protein and on a C-terminal N-Ras peptide. *J. Biol. Chem.* **271**, 23269-23276.

Liu, J., Hughes, T. E. and Sessa, W. C. (1997). The first 35 amino acids and fatty acylation sites determine the molecular targeting of endothelial nitric oxide synthase into the Golgi region of cells: a green fluorescent protein study. *J. Cell Biol.* **137**, 1525-1535.

Luetterforst, R., Stang, E., Zorzi, N., Carozzi, A., Way, M. and Parton, R. G. (1999). Molecular characterization of caveolin association with the Golgi complex: identification of a cis-Golgi targeting domain in the caveolin molecule. *J. Cell Biol.* **145**, 1443-1459.

Martín-Belmonte, F., López-Guerrero, J. A., Carrasco, L. and Alonso, M. A. (2000). The N-terminal nine amino acid sequences of poliovirus capsid VP4 protein is sufficient to confer N-myristoylation and targeting to detergent-insoluble membranes. *Biochemistry* **39**, 1083-1090.

McCabe, J. B. and Berthiaume, L. G. (1999). Functional roles for fatty acylated amino-terminal domains in subcellular localization. *Mol. Biol. Cell* **10**, 3771-3786.

McCabe, J. B. and Berthiaume, L. G. (2001). N-terminal protein acylation confers localization to cholesterol, sphingolipid-enriched membranes but not to lipid rafts/caveolae. *Mol. Biol. Cell* **12**, 3601-3617.

Melkonian, K. A., Ostermeyer, A. G., Chen, J. Z., Roth, M. G. and Brown, D. A. (1999). Role of lipid modifications in targeting proteins to detergent-resistant membrane rafts. Many raft proteins are acylated, while few are prenylated. *J. Biol. Chem.* **274**, 3910-3917.

Michaelson, D., Silletti, J., Murphy, G., D'Eustachio, P., Rush, M. and Philips, M. R. (2001). Differential localization of Rho GTPases in live cells: regulation by hypervariable regions and RhoGDI binding. *J. Cell Biol.* **152**, 111-126.

Milligan, G., Parenti, M. and Magee, A. I. (1995). The dynamic role of palmitoylation in signal transduction. *Trends Biochem Sci.* **20**, 181-187.

Mollner, S., Ferreira, P., Beck, K. and Pfeuffer, T. (1998). Nonenzymatic palmitoylation at Cys 3 causes extra-activation of the alpha-subunit of the stimulatory GTP-binding protein Gs. *Eur. J. Biochem.* **257**, 236-241.

Nusrat, A., Parkos, C. A., Verkade, P., Foley, C. S., Liang, T. W., Innis-Whitehouse, W., Eastburn, K. K. and Madara, J. L. (2000). Tight junctions are membrane microdomains. *J. Cell. Sci.* **113**, 1771-1781.

O'Brien, P. J., St Jules, R. S., Reddy, T. S., Bazan, N. G. and Zatz, M. (1987). Acylation of disc membrane rhodopsin may be nonenzymatic. *J. Biol. Chem.* **262**, 5210-5215.

Peitzsch, R. M. and McLaughlin, S. (1993). Binding of acylated peptides and fatty acids to phospholipid vesicles: pertinence to myristoylated proteins. *Biochemistry* **32**, 10436-10443.

Pepinsky, R. B., Zeng, C., Wen, D., Rayhorn, P., Baker, D. P., Williams, K. P., Bixler, S. A., Ambrose, C. M., Garber, E. A., Miatkowski, K. et al. (1998). Identification of a palmitic acid-modified form of human Sonic hedgehog. *J. Biol. Chem.* **273**, 14037-14045.

Quesnel, S. and Silvius, J. R. (1994). Cysteine-containing peptide sequences exhibit facile uncatalyzed transacylation and acyl-CoA-dependent acylation at the lipid bilayer interface. *Biochemistry* **33**, 13340-13348.

Resh, M. D. (1994). Myristylation and palmitylation of Src family members: the fats of the matter. *Cell* **76**, 411-413.

Resh, M. D. (1999). Fatty acylation of proteins: new insights into membrane targeting of myristoylated and palmitoylated proteins. *Biochim. Biophys. Acta.* **1451**, 1-16.

Robinson, L. J., Busconi, L. and Michel, T. (1995). Agonist-modulated palmitoylation of endothelial nitric oxide synthase. *J. Biol. Chem.* **270**, 995-998.

Schmidt, M. F., McIlhinney, R. A. and Burns, G. R. (1995). Palmitoylation of endogenous and viral acceptor proteins by fatty acyltransferase (PAT) present in erythrocyte ghosts and in placental membranes. *Biochim. Biophys. Acta.* **1257**, 205-213.

Simons, K. and Toomre, D. (2000). Lipid rafts and signal transduction. *Nat. Rev. Mol. Cell. Biol.* **1**, 31-39.

ten Brinke, A., Vaandrager, A. B., Haagsman, H. P., Ridder, A. N., van Golde, L. M. and Batenburg, J. J. (2002). Structural requirements for palmitoylation of surfactant protein C precursor. *Biochem. J.* **361**, 663-671.

Ueno, K. and Suzuki, Y. (1997). p260/270 expressed in embryonic abdominal leg cells of Bombyx mori can transfer palmitate to peptides. *J. Biol. Chem.* **272**, 13519-13526.

van't Hof, W. and Resh, M. D. (2000). Targeting proteins to plasma membrane and membrane microdomains by N-terminal myristoylation and palmitoylation. *Methods Enzymol.* **327**, 317-330.

Veit, M., Sachs, K., Heckelmann, M., Maretzki, D., Hofmann, K. P. and Schmidt, M. F. (1998). Palmitoylation of rhodopsin with S-protein acyltransferase: enzyme catalyzed reaction versus autocatalytic acylation. *Biochim. Biophys. Acta.* **1394**, 90-98.

Webb, Y., Hermida-Matsumoto, L. and Resh, M. D. (2000). Inhibition of protein palmitoylation, raft localization, and T cell signaling by 2-bromopalmitate and polyunsaturated fatty acids. *J. Biol. Chem.* **275**, 261-270.

Wedegaertner, P. B., Wilson, P. T. and Bourne, H. R. (1995). Lipid modifications of trimeric G proteins. *J. Biol. Chem.* **270**, 503-506.

Yamashita, A., Watanabe, M., Tonegawa, T., Sugiura, T. and Waku, K. (1995). Acyl-CoA binding and acylation of UDP-glucuronosyltransferase isoforms of rat liver: their effect on enzyme activity. *Biochem. J.* **312**, 301-308.

Yeh, D. C., Duncan, J. A., Yamashita, S. and Michel, T. (1999). Depalmitoylation of endothelial nitric-oxide synthase by acyl-protein thioesterase 1 is potentiated by Ca(2+)-calmodulin. *J. Biol. Chem.* **274**, 33148-33154.